International Journal of Engineering Research & Technology (IJERT)
ISSN: 2278-0181
Vol. 15 Issue 05 , May - 2026

Numerical Analysis on Cyclic Static Loading Behaviour of Hollow UHPC Encased Inverted T Steel Composite Beams

Hithesh Mangalat
Master's Student, Computer Aided Structural Engineering
Department of Civil Engineering
Government College of Engineering, Kannur
Kerala, India

Dr. Narayanan N. I.
Assistant Professor
Department of Civil Engineering
Government College of Engineering, Kannur
Kerala, India

Abstract **- The rapid development of modern infrastructure demands structural systems that are lightweight, durable, sustainable, and capable of resisting complex loading conditions. This study investigates the cyclic performance of a Precast Ultra-High Performance Concrete (UHPC) Encased Inverted T-Steel (PUES) composite beam with hollow sections. UHPC enhances the composite system by providing high strength, improved crack resistance, and superior durability compared to conventional concrete systems. A detailed finite element model was developed in ABAQUS using the Concrete Damaged Plasticity (CDP) model and validated with experimental results under monotonic loading. After validation, displacement-controlled cyclic loading was applied to evaluate load–deflection behaviour, hysteresis response, energy dissipation, stiffness degradation, and crack propagation. The study compares hollow and solid PUES beam configurations under identical cyclic loading conditions. Results show that hollow PUES beams achieve significant reduction in self-weight and material usage while maintaining satisfactory cyclic performance. Although hollow beams exhibited slightly earlier stiffness degradation and localized stress concentrations, their overall ductility, hysteretic behaviour, and energy dissipation remained comparable to solid beams. Among all specimens, PUES-2 demonstrated superior performance with higher load-carrying capacity, improved stiffness retention, and nearly 18–22% greater cumulative energy dissipation. The findings confirm the structural feasibility of hollow PUES beams for lightweight and sustainable applications in bridges, modular construction, high-rise buildings, and seismic-resistant structures.**

Keywords **-** ***UHPC composite beam, PUES, steel–UHPC composite system, finite element analysis, Concrete Damaged Plasticity, cyclic loading, hysteresis behaviour***

I. INTRODUCTION

Composite construction has long been recognized as an efficient means of utilizing the complementary properties of steel and concrete. Steel concrete composite beams are extensively used in bridge and building structures due to their high strength, ductility, and rapid construction capability [1][2]. Steel provides high tensile strength and ductility, while concrete contributes excellent compressive strength and stiffness. When these two materials are combined appropriately, they yield structures with enhanced performance, lower self-weight, and improved durability compared with monolithic systems.

In the pursuit of more sustainable and economical construction, the use of advanced materials such as Ultra-High-Performance Concrete (UHPC) has become increasingly attractive [3]. UHPC possesses superior mechanical characteristics compressive strengths typically above 150 MPa, tensile strength up to 12 MPa with fibres, and extremely low permeability making it suitable for long-span bridges, precast girders, and heavily loaded floor systems. Despite these advantages, the uniform use of UHPC throughout a section often leads to unnecessary material consumption and high cost, motivating exploration into material gradation techniques. The unique crack control capability ensures superior durability and makes UHPC highly suitable for composite structural applications. To efficiently utilize the superior mechanical properties of UHPC while reducing material cost, Gao et al. (2024) proposed an innovative composite beam known as the Precast UHPC Encased Inverted T-Steel (PUES) beam with hollow section. The concept integrates an inverted T-shaped steel section with a peripheral UHPC shell and a cast-in-place UHPC layer to form a highly efficient steel UHPC composite system [3]. studies have shown that the cracking load of such beams is only 14–40% of the ultimate load, leaving a significant risk of premature damage. To address this limitation, the study introduces a new perfobond rib shear (PBL) connector wrapped with foam plastic, designed to release tensile stresses and improve cracking resistance. This innovation forms the central motivation of the research, aiming to enhance the performance of steel–UHPC composite beams under negative bending moments [2].

II. AIM, OBJECTIVE AND SCOPE

The aim of this project is to develop and validate a detailed ABAQUS finite element model of the PUES hollow inverted T steel UHPC composite beam and to investigate its cyclic flexural behaviour using Concrete Damaged Plasticity for UHPC and cohesive steel UHPC interface

International Journal of Engineering Research & Technology (IJERT)
ISSN: 2278-0181
Vol. 15 Issue 05 , May - 2026

modelling, with emphasis on damage evolution, stiffness degradation, energy dissipation, and composite action under displacement-controlled reversed loading.

The primary objective of this study is to investigate the cyclic structural behaviour of Precast Ultra-High Performance Concrete (UHPC) Encased Inverted T-steel (PUES) composite beams using finite element analysis in ABAQUS. The study aims to extract the geometry, material properties, and experimental test details of PUES-1 to PUES-4 from the reference experimental work and accurately reproduce them in the numerical model. UHPC is modelled using the Concrete Damaged Plasticity (CDP) approach to realistically capture crack propagation and crushing behaviour observed in experiments, while the inverted-T steel section and stud connectors are modelled to simulate effective composite interaction. The developed finite element model is validated by comparing load–deflection response, crack patterns, failure modes, and ultimate load with available experimental results. After validation under monotonic loading, the loading protocol is replaced with displacement-controlled cyclic loading to generate hysteresis behaviour. The study further evaluates stiffness degradation, strength degradation, and energy dissipation characteristics under repeated loading cycles. In addition, damage evolution in UHPC through tensile and compressive damage parameters (dt and dc), plastic hinge formation, and neutral axis migration during cyclic loading are investigated. Finally, the cyclic performance of solid and hollow PUES beam configurations is compared to assess the feasibility of lightweight hollow composite systems for sustainable structural applications.

The present study is confined to a detailed numerical investigation using ABAQUS based on the reference PUES experimental beam configuration. Initially, the finite element model is developed and validated using the monotonic test results reported in the experimental study, ensuring that the numerical model accurately reproduces the load–deflection behaviour, crack pattern, and failure mode observed in the tests. Once validated, the same model is subjected to displacement controlled cyclic static loading to simulate realistic reversed loading conditions. The study focuses on extracting key behavioural parameters such as hysteresis loops, stiffness degradation, energy dissipation capacity, damage evolution contours, neutral axis shift. In addition, a comparison between solid and hollow PUES beam configurations is performed under identical cyclic loading conditions to evaluate the structural efficiency of the hollow concept. The overall aim is to establish a numerically validated modelling framework and to provide a comprehensive performance assessment of steel–UHPC composite beams under cyclic flexure.

III. METHODOLOGY AND MODELLING

The present study adopts a nonlinear finite element–based numerical methodology to investigate the cyclic static behaviour of an Inverted-T steel–UHPC composite beam developed from the PUES concept. Because experimental testing of UHPC composite members under cyclic loading is complex and resource-intensive, ABAQUS is employed to simulate the response with high fidelity. The beam, supports are modelled using three-dimensional continuum elements with nonlinear geometry (NLGEOM) enabled to capture large deformations. UHPC is represented through the Concrete Damage Plasticity (CDP) model to simulate tensile cracking, compressive crushing, stiffness degradation, and damage evolution during load reversals. The inverted-T steel section is defined using material model to capture yielding and plastic strain development. Surface-to-surface contact interactions are used instead of tie constraints to permit separation and sliding at interfaces, thereby reproducing realistic composite action. A displacement-controlled cyclic loading approach is adopted through a tabular amplitude to generate hysteresis behaviour, enabling the study of stiffness degradation and energy dissipation. Mesh refinement is applied near critical regions such as loading points, supports, and material interfaces to ensure numerical accuracy and stability.

The numerical procedure begins with the creation of three-dimensional geometries of the UHPC slab, embedded inverted-T steel section, supports and loading parts according to the dimensions reported in the reference study for two different beams. Material properties are then assigned, with UHPC defined using CDP parameters, steel properties are assigned as per the reference literature. After section assignment, all components are assembled in their exact spatial positions to form the composite beam setup.
For validation, the first beam is analysed under monotonic displacement loading identical to the experimental setup. Reaction force and mid-span displacement are extracted to generate the load– deflection curve, which is compared with the experimental results. After satisfactory agreement is obtained, the same steps are repeated for the second beam. Necessary minor adjustments in mesh density and contact stabilization are performed to achieve convergence without altering material behaviour. This confirms the robustness of the modelling approach.
After validating beam, cyclic displacement loading is applied at the mid-span through a tabular amplitude, reaching a maximum displacement of 36 mm within a total step time of one unit. The analysis is executed while monitoring convergence behaviour. Finally, results are postprocessed to generate hysteresis curves, visualize damage progression, and evaluate stiffness degradation and energy dissipation characteristics of the composite beam.

The geometry of the PUES beam consists of a steel I-section combined with a UHPC slab to form a composite member. The steel beam is placed below the UHPC slab and connected using headed stud shear connectors to ensure composite action between the two materials. The cross-sectional dimensions, including flange width, web thickness, slab thickness, and stud spacing of the beam are shown in Fig.1 and in Fig 2.

International Journal of Engineering Research & Technology (IJERT)
ISSN: 2278-0181
Vol. 15 Issue 05 , May - 2026

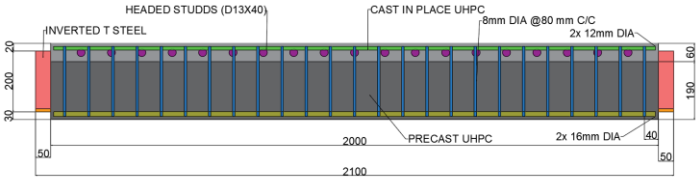

Fig. 1 Detailed scheme for the test specimen

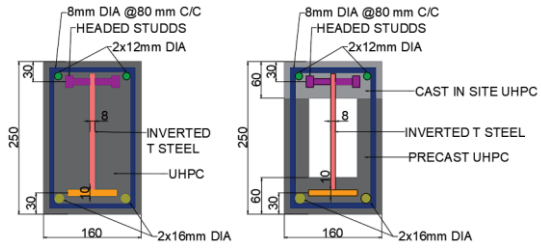

Fig. 2 Detailed section scheme for test specimen

A. Material properties of the beam

The PUES beam is composed of UHPC, structural steel, and headed stud shear connectors, each contributing to the overall structural performance. UHPC is characterized by very high compressive strength, improved tensile resistance due to the presence of steel fibers, and a dense microstructure that enhances durability and stiffness. It primarily resists compressive stresses in the composite beam and provides high initial stiffness. Structural steel exhibits a linear elastic behaviour up to its yield strength, followed by a ductile plastic region that allows large deformations without sudden failure. This ductility enables the formation of plastic hinges and ensures stable post-yield behaviour. The headed stud shear connectors provide the necessary bond between the steel beam and the UHPC slab, allowing effective transfer of shear forces and ensuring composite action. The combined properties of high-strength UHPC and ductile steel result in a beam with enhanced flexural capacity, stiffness, and deformation capacity. The materials properties of UHPC are shown in table 1. The material properties of steel and rebar are shown in table 2.

Table 1 Mechanical Properties Of UHPC

Mechanical Properties Of UHPC				
Casting Batch	**Cubic Compressive Strength(MPa)**	**Elastic Tensile Strength(MPa)**	**Ultimate Tensile Strength(MPa)**	**Elastic Modulus(GPa)**
Precast UHPC	125.9	7.9	8.9	43.6
Cast-In-Place UHPC	123.8	8.1	9.2	42.8

Table 2 Mechanical properties of steel shape and steel rebar

Mechanical Properties Of Steel Shape And Steel Rebar					
Type	**Thickness (mm)**	**Diameter (mm)**	**Yield Strength (Mpa)**	**Ultimate Strength (Mpa)**	**Elastic Modulus(Gpa)**
Steel Shape	8		474	625	205
	10		508	589	210
Steel Rebar		8	448	652	203
		12	526	601	206
		16	489	625	204

The tensile and compressive deformation behaviour of concrete is simulated by the Concrete Damage Plasticity (CDP) model in GB50010-2010. The CDP model considers that the damage modes of concrete are divided into two types, tensile cracking and compressive crushing, and puts the concrete into the plastic state through a reduction in the stiffness related to the plastic strain of the concrete and the tensile and compressive damage factors, which can effectively simulate the stiffness change of concrete structures under loading [26][27]. In the Abaqus software, the CDP model can be calculated through the basic parameters: the ratio of biaxial strength σbo compared with uniaxial strength σco in compression, the failure surface k_c, dilation angle ϕ, eccentricity ξ and the viscosity μ. Table 3 shows the parameters of the CDP model in the simulation model [28].

Table 3. CDP model for UHPC material in Abaqus

Element	**Value**
Dilation Angle	37
Eccentricity	0.1
fb_0/fc_0	1.16
K	0.67
Viscosity Parameter	0.0005

The contact conditions of the FEM model are presented in Table 4. The surface-to surface contact provided in ABAQUS was taken into account to define the interactions of the contact pairs. Generally, the contact pairs included the steel beam-to-UHPC and reinforcement and the head stud-to-concrete. For the former contact pairs, the surfaces of the steel components

International Journal of Engineering Research & Technology (IJERT)
ISSN: 2278-0181
Vol. 15 Issue 05 , May - 2026

were regarded as the master surface, and the corresponding concrete surfaces were selected as slave surfaces.

Table 4 Interactions

Models	Interactions
UHPC-Reinforcement	Embedded Region
UHPC-Tsteel	Embedded Region
Studds-Tsteel	Tie
Studds-UHPC	Embedded Region
Support-Beam	Surface to Surface Contact

The complete meshed model is as shown below in Fig. 3 (a) and (b). The finite element modelling of inverted T steel-concrete composite beams in ABAQUS requires careful consideration of interactions between different materials and proper boundary condition definitions to simulate realistic structural behaviour. The fundamental modelling challenge involves accurately representing the interaction between dissimilar materials are shown in Table 5 (steel, concrete, reinforcement, and shear connectors) and defining appropriate boundary conditions that replicate simply supported behaviour in experimental or real-world conditions. The element type and mesh size used for each models are shown in table 5.

Table 5 Element type and Mesh size

Model	Element type	Mesh size (mm)
UHPC	C3D8R	25
Tsteel	C3D8R	25
Support	R3D4	25
Studds	C3D8R	8
Stirrup	T3D2	8
Rebar 12	T3D2	12
Rebar16	T3D2	16

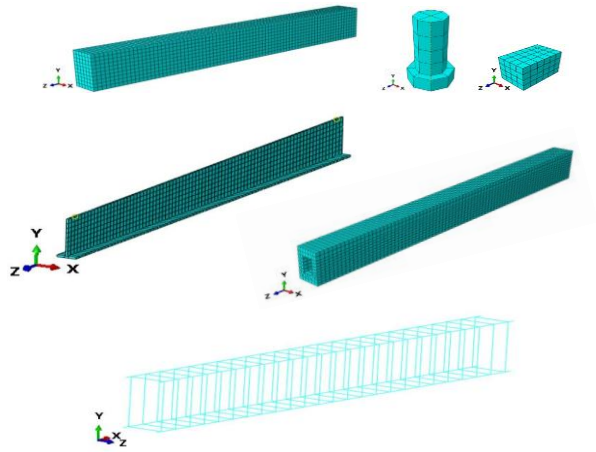

- Fig. 3 (a) Meshed Models

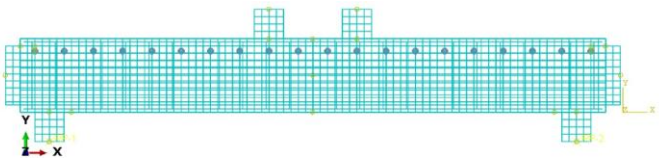

- Fig. 3 (b) Meshed Models

The beam geometry was defined according to the experimental dimensions, including span length, cross-sectional size, and reinforcement detailing. Concrete was modelled as a three-dimensional continuum solid to enable realistic simulation of cracking, crushing, and nonlinear stress redistribution. Reinforcement was incorporated within the concrete domain to represent longitudinal bars and stirrups contributing to flexural and shear resistance.

Material behaviour was defined using nonlinear constitutive relationships. Concrete behaviour was represented using a damage plasticity based model capable of capturing tensile cracking and compressive crushing. The model accounts for stiffness degradation under increasing strain through scalar damage variables in tension and compression. Reinforcement steel was modelled using an elastic–plastic material law with strain hardening, enabling simulation of yielding and post-yield behaviour.

The analysis incorporated geometric nonlinearity to account for large displacement effects where necessary. This allows accurate prediction of deflection behaviour and post-yield response, particularly under cyclic or impact loading.

IV. VALIDATION

Validation is the process of verifying that a finite element model accurately represents the real structural behaviour observed in experiments or established analytical solutions. In beam modelling using ABAQUS, validation ensures that the numerical simulation reliably predicts stiffness, strength, cracking behaviour, ductility, and energy dissipation characteristics. The developed finite element model was validated by comparing the numerical results obtained from ABAQUS with the experimental results reported by Gao et al. (2024) [1]. The validation process was carried out to ensure the accuracy and

International Journal of Engineering Research & Technology (IJERT)
ISSN: 2278-0181
Vol. 15 Issue 05 , May - 2026

reliability of the numerical model in predicting the flexural behaviour of UHPC composite beams with inverted T-shaped steel sections.
The UHPC material was modelled using the Concrete Damage Plasticity (CDP) model, while steel components were modelled using elastoplastic material behaviour. Surface-to-surface interactions and embedded constraints were used to simulate realistic composite action between UHPC, reinforcement, shear studs, and the inverted T-steel section. A validated model provides confidence that subsequent parametric studies, impact simulations, or design modifications are scientifically meaningful and structurally reliable.

Validation is performed by comparing numerical results with experimental data using key structural response parameters. The most fundamental validation parameter is the load– deflection curve. The load–deflection response obtained from the FE analysis of beam 1 as shown in Figure 4 showed good agreement with the experimental results throughout the loading stages. The FE model accurately captured the elastic behaviour, stiffness characteristics, and nonlinear response up to failure. The table shows the percentage error of experimental and numerical results of beam 1. Table 6 shows the error of experimental and numerical results.

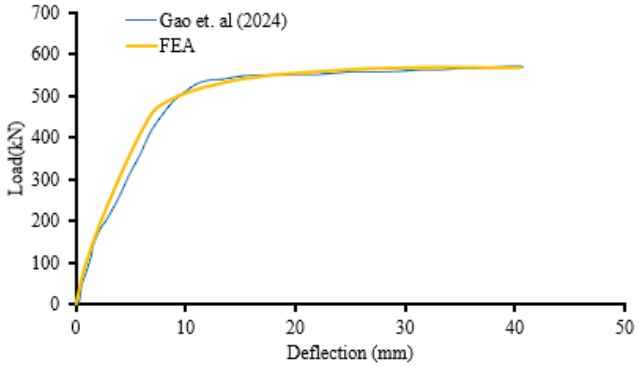

Fig. 4 Load deflection response of Beam 1

Table 6: % error of experimental and numerical results (beam 1)

Parameter	Experimental	FEA	Error (%)
Ultimate Load (kN)	550	556	1.09
Deflection at Ultimate Load (mm)	19	20	5.26
Initial Stiffness (kN/mm)	64.3	67.1	4.35

The FE model predicted the ultimate load with only 1.09% error, indicating excellent agreement with the experimental behaviour. The initial stiffness was also accurately captured with an error of 4.35%.

The numerical load–deflection curve as shown in Figure 5 for validation Specimen 2 closely matched the experimental response. The FE model successfully predicted the nonlinear flexural behaviour and stiffness characteristics of the beam. The table shows the percentage error of experimental and numerical results of beam 2. Table 7 shows the error of experimental and numerical results.

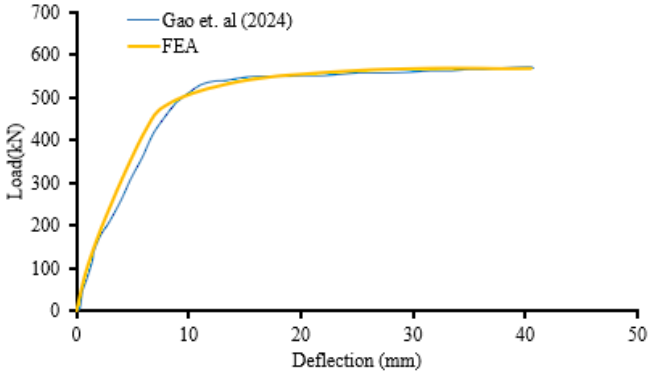

Fig. 5 Load deflection response of Beam 2

Table 7: % error of experimental and numerical results (beam 2)

Parameter	Experimental	FEA	Error (%)
Ultimate Load (kN)	544	565	3.86
Deflection at Ultimate Load (mm)	16	17	6.25
Initial Stiffness (kN/mm)	64.3	67.1	4.35

The FE analysis predicted the ultimate load with an error of 3.86%, while the deflection at ultimate load showed an error of 6.25%. These values confirm the capability of the FE model to reproduce the experimental flexural response with acceptable accuracy.

A quantitative comparison between the experimental and numerical load–deflection curves was performed. The overall percentage error was calculated within 10% for all the specimen. The deviation remains within the acceptable range (< 15 %) for nonlinear concrete simulations using the CDP model, confirming the reliability of the developed finite element model. The validation results confirm the reliability and accuracy of the developed finite element model for

International Journal of Engineering Research & Technology (IJERT)
ISSN: 2278-0181
Vol. 15 Issue 05 , May - 2026

studying the cyclic performance, stiffness degradation, damping characteristics, and energy dissipation behaviour of UHPC composite beams.

V. RESULTS AND DISCUSSION

A quasi-static displacement-controlled cyclic load was applied at one end of the beam specimen through a reference point coupled to the loading plate. The cyclic loading history was defined using a predefined amplitude function to simulate reversed loading conditions. The analysis was conducted under displacement control to ensure stable post-yield response and to accurately capture stiffness degradation and energy dissipation behaviour.

The loading protocol consisted of increasing displacement amplitudes in both positive and negative directions. Each displacement level was repeated two times before yielding, three cycles after yielding and continuing displacement amplitudes until degradation to evaluate strength deterioration, stiffness degradation, and damage accumulation under recurring loading. The cyclic amplitudes were selected based on the expected yield displacement of the beam and were increased incrementally to reach the target ultimate displacement [29].

The loading rate was chosen to ensure quasi-static conditions, minimizing inertial effects during the analysis. The applied displacement history was defined in tabular form within the amplitude definition, enabling symmetric forward and reverse loading paths. The boundary conditions were assigned to replicate the experimental support configuration, and all nonlinear effects, including material nonlinearity and geometric nonlinearity, were considered in the analysis.

This cyclic loading setup enables detailed evaluation of hysteretic behaviour, energy dissipation capacity, and ductility performance of the beam under simulated seismic-type loading. Fig. 5 shows the cyclic loading applied to the beam.

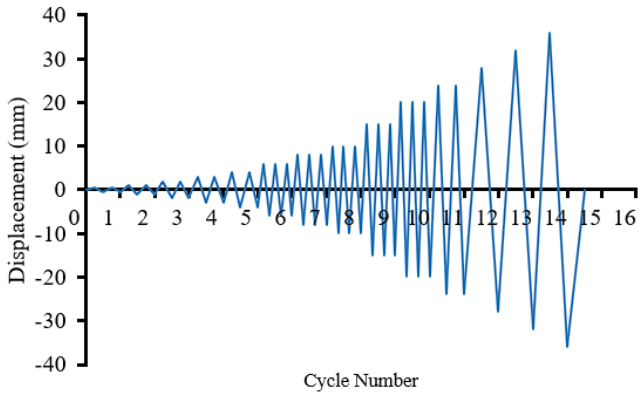

Fig, 5 Cyclic Loading

A. *hysteresis behaviour of composite beams*

Beam B1 consisted of a solid UHPC section reinforced with 16 mm bottom reinforcement. Figure 6 shows the hysteresis response of B1 showed stable cyclic behaviour with comparatively narrow hysteresis loops during the initial cycles. As loading progressed, the loops widened gradually due to increased inelastic deformation.

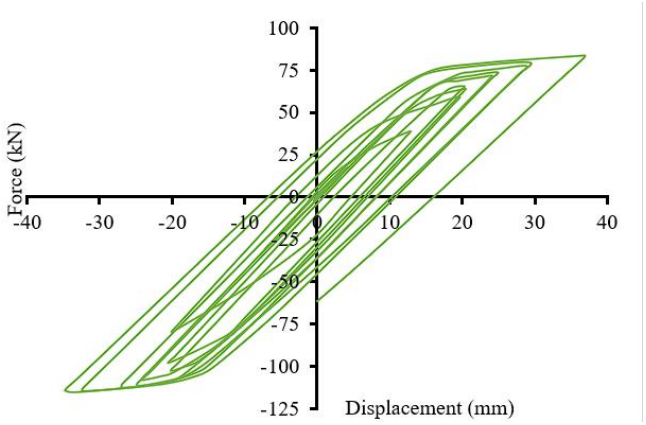

Fig 6 Hysteresis response of B1

The beam exhibited:

- Stable load carrying capacity throughout the loading cycles
- Gradual stiffness degradation
- Good resistance against excessive deformation
- Controlled crack propagation

The solid section provided improved structural continuity and higher residual stiffness during repeated loading cycles. The hysteresis loops remained relatively stable even at higher displacement amplitudes, indicating strong cyclic stability. The stress and damage distribution obtained from the ABAQUS finite element analysis as shown in figure 7, 8, 9 and 10 respectively illustrates the structural response of the beam under cyclic loading conditions. The contour plots help identify the regions of maximum stress concentration, crack initiation and progressive material failure during loading cycles.

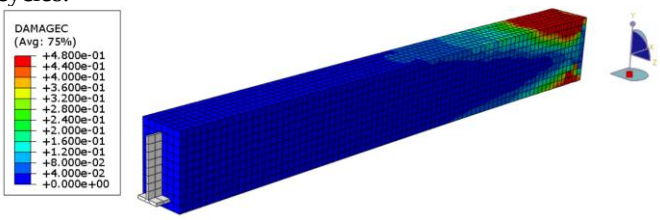

Fig 7. Compression damage (beam 1)

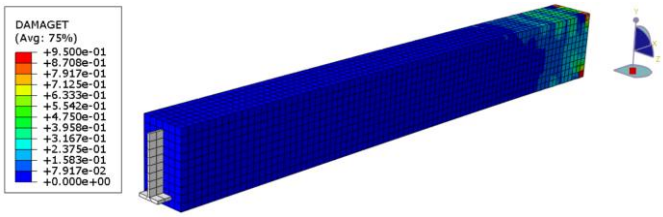

Fig 8. Tension damage (beam 1)

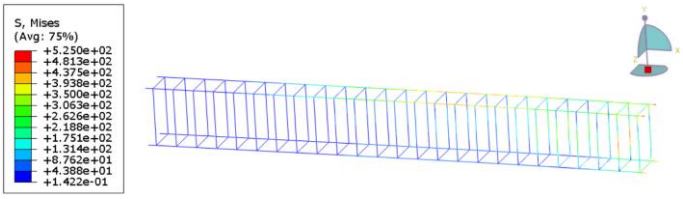

Fig 9 Stress in reinforcement (beam 1)

International Journal of Engineering Research & Technology (IJERT)
ISSN: 2278-0181
Vol. 15 Issue 05 , May - 2026

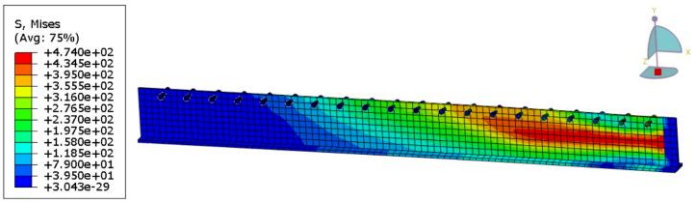

Fig 10 Stress in inverted T steel with shear studs (beam 1)

The compression and tension damage contours showed progressive damage concentration near the loading region and tensile zones. However, damage propagation remained controlled because of the high compressive strength and ductility of UHPC.
The stress distribution in the inverted T-steel section and reinforcement indicated effective composite interaction between steel and UHPC.

Beam B2 consisted of a hollow UHPC section reinforced with 16 mm bottom reinforcement. Compared with B1, the hollow section reduced the overall self-weight while maintaining effective cyclic performance. Figure 11 shows the hysteresis response of B2

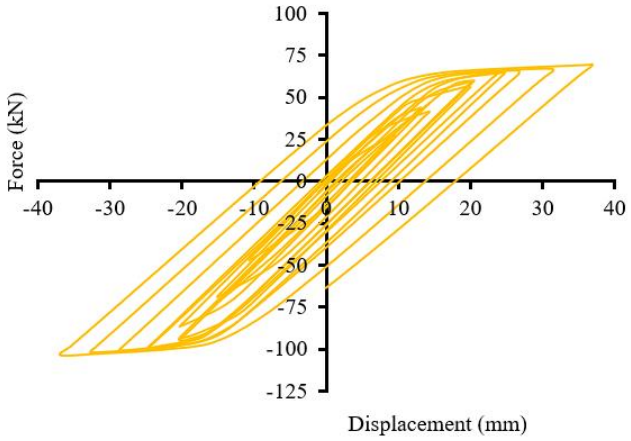

Fig 11 Hysteresis response of B2

The hysteresis behaviour of B2 demonstrated:

- Improved initial energy dissipation
- Higher damping characteristics during early loading cycles
- Increased hysteretic loop area in later cycles
- Faster stiffness degradation after repeated loading

The hollow section promoted slightly higher ductility and deformation capacity. During the initial loading stages, B2 exhibited better energy absorption than the solid beam due to increased flexibility.
However, as cyclic loading increased, the hollow section experienced faster stiffness degradation because of reduced sectional rigidity. Despite this, the beam maintained adequate load carrying capacity and stable hysteresis behaviour. The stress and damage distribution obtained from the ABAQUS finite element analysis as shown in Figure 12, 13, 14 and 15 respectively illustrates the structural response of the beam under cyclic loading conditions. The contour plots help identify the regions of maximum stress concentration, crack initiation and progressive material failure during loading cycles.

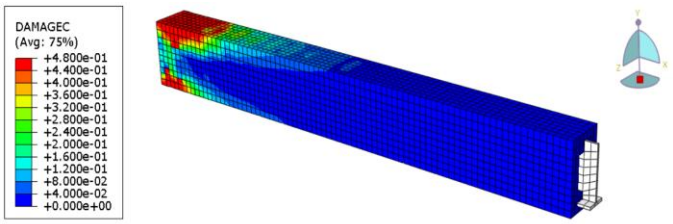

Fig 12. Compression damage (beam 2)

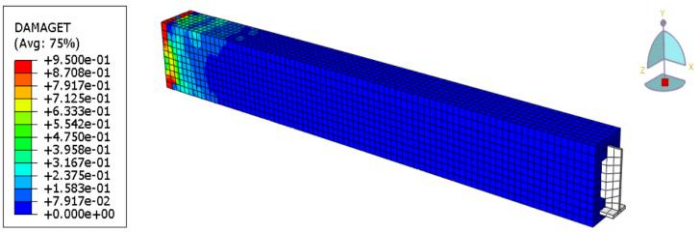

Fig 13. Tension damage (beam 2)

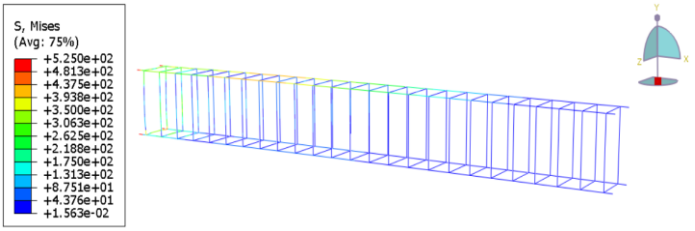

Fig 14 Stress in reinforcement (beam 2)

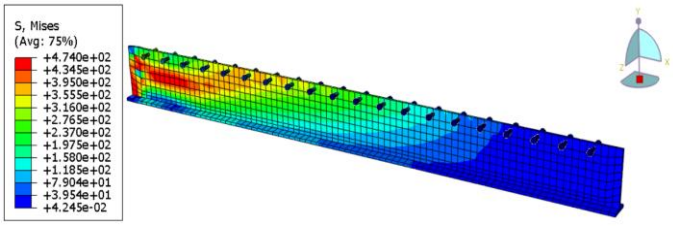

Fig 15 Stress in inverted T steel with shear studs (beam 2)

The stress contours revealed that stresses were effectively transferred between the UHPC section, steel beam, and reinforcement. Localized damage accumulation occurred near the tensile region and around stress concentration zones.

B. . Energy dissipation behaviour

Energy dissipation is one of the most important parameters in evaluating cyclic structural performance. It represents the ability of a structure to absorb and dissipate energy during repeated loading. The energy dissipation graph for B1 and B2 is shown in Figure 16. The energy dissipation per cycle is defined as $E_d = \int (P \times d\Delta)$, Where P is the maximum load and $d\Delta$ is the maximum deflection in each cycle.

International Journal of Engineering Research & Technology (IJERT)
ISSN: 2278-0181
Vol. 15 Issue 05 , May - 2026

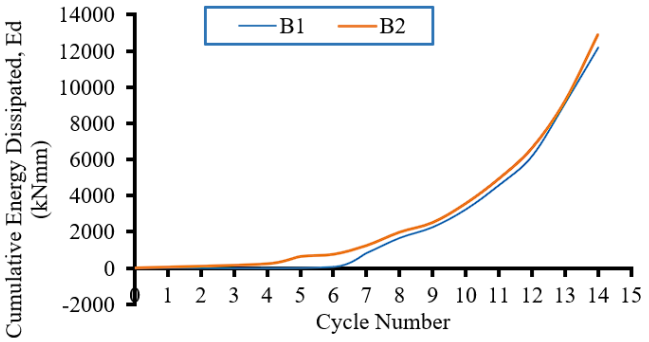

Fig. 16 Cummulative Energy Dissipation Curve

1) Behaviour of Beam B1

The solid section beam demonstrated stable and progressive energy dissipation throughout the loading cycles. The energy dissipation increased steadily because of gradual plastic deformation and controlled damage propagation.

The solid section provided:

- Better stiffness retention
- Stable cyclic response
- Reduced deformation concentration
- Improved long-term structural stability

However, the energy dissipation capacity during the initial loading cycles was slightly lower compared to the hollow beam. From the cumulative energy dissipation graph, Beam B1 reached approximately 11,800–12,000 kNmm during the final loading cycle. The increase in energy dissipation was gradual and stable throughout all 15 loading cycles, indicating controlled hysteretic behaviour and better long-term cyclic stability.

2) Behaviour of Beam B2

Beam B2 exhibited slightly higher energy dissipation during the initial cycles. The hollow section increased flexibility, which enhanced deformation capability and hysteretic energy absorption.

At higher loading cycles, the cumulative energy dissipation increased sharply because of:

- Increased plastic deformation
- Crack propagation
- Damage accumulation
- Enhanced hysteretic response

The final cumulative energy dissipation of B2 was marginally higher than B1, indicating improved ductility and cyclic energy absorption. Beam B2 achieved approximately 12,500–13,000 kNmm cumulative energy dissipation during the final loading cycle, which was slightly higher than Beam B1. During the initial cycles, B2 also showed faster energy dissipation growth because of increased flexibility and deformation capability.

3) Comparative Discussion

The comparison between B1 and B2 indicates that:

- Hollow sections improve initial cyclic energy dissipation.
- Solid sections provide better long-term stiffness stability.
- Hollow beams exhibit higher flexibility and ductility.
- Solid beams resist degradation more effectively during prolonged loading.

Therefore, hollow UHPC sections can achieve effective cyclic energy absorption while reducing self-weight.

VI. CONCLUSION

The overall results obtained from the nonlinear finite element analysis demonstrate that UHPC composite beams possess excellent cyclic performance due to the combined advantages of UHPC material properties and steel composite action. The study confirms that UHPC significantly improves crack resistance and structural durability, while inverted T-steel sections enhance flexural strength and stiffness. Hollow sections were found to effectively reduce self-weight while still maintaining satisfactory cyclic performance, and larger reinforcement ratios contributed to improved cyclic stability, energy dissipation, and damping characteristics. In addition, the composite interaction between steel and UHPC enhanced the overall structural efficiency of the beams. The cyclic analysis showed that all beam specimens were capable of sustaining repeated loading with progressive hysteretic energy dissipation and controlled damage propagation. A comparison between solid and hollow sections revealed that hollow UHPC beams provided better initial energy dissipation, improved damping behaviour, reduced structural self-weight, and increased deformation flexibility. However, solid sections retained residual stiffness more effectively during prolonged cyclic loading..

VII. ACKNOWLEDGMENT

I would like to express my sincere gratitude to the organization for their valuable contributions for this work. I would also extend appreciation to Dr. Narayanan N. I. who provided technical support and guidance throughout the process.

REFERENCES

[I] Gao, X., Wang, M., Guo, J., & Li, H. (2024). Flexural behaviors of a novel precast hollow UHPC composite beam reinforced with inverted T-shaped steel: Experimental investigation and theoretical analysis. Journal of Building Engineering, 86, 108893. https://doi.org/10.1016/j.jobe.2024.108893

[II] Mao, M., Yin, C., Shen, S., & Wan, Y. (2024). Experimental and Numerical Study on Flexural Behaviors of SteelUHPC Composite Beams under Hogging Moment. KSCE Journal of Civil Engineering, 28(6), 2344–2354.

[III] Zhang, Y., Wang, H., Qin, Y., Huang, S., & Fan, W. (2023). Experimental and analytical studies on the flexural behavior of steel plate-UHPC composite strengthened RC beams. Engineering Structures, 283, 115834. https://doi.org/10.1016/j.engstruct.2023.115834

[IV] Abbas, E. M., Ge, Y., Zhang, Z., Chen, Y., Ashour, A., Ge, W., Tang, R., Yang, Z., Khailah, E. Y., Yao, S., & Sun, (2022). Flexural behavior of UHPC beam reinforced with steel-FRP composite bars. Case Studies in Construction Materials, 16, e01110. https://doi.org/10.1016/j.cscm.2022.e01110

[V] Xinghong, J., Ke, L., Min, L., Yongwei, W., Yongkang, W., & Lihua, S. (2023). Flexural performance test and finite element analysis of UHPC-NC composite beam. Case Studies in Construction Materials, 20, e02771. https://doi.org/10.1016/j.cscm.2023.e02771

[VI] Ge, W., Liu, C., Zhang, Z., Guan, Z., Ashour, A., Song, S., Jiang, H., Sun, C., Qiu, L., Yao, S., Yan, W., & Cao, (2022). Numerical and theoretical research on flexural behaviour of steel-precast UHPC composite beams. Case Studies in Construction Materials, 18, e01789. https://doi.org/10.1016/j.cscm.2022.e01789

International Journal of Engineering Research & Technology (IJERT)
ISSN: 2278-0181
Vol. 15 Issue 05 , May - 2026

[VII] Wu, C., Wang, X., Zhang, Z., Zou, Y., Yang, J., Jin, M., & Lun, X. (2024). Flexural behavior of embedded GFRP grid framework-UHPC composite plate without steel rebar. Case Studies in Construction Materials, 20, e02900. https://doi.org/10.1016/j.cscm.2024.e02900

[VIII] Li, H., Li, L., Du, C., Ye, M., Shao, X., & Zhou, C. (2023). Experimental Study on the Flexural Behavior of a Novel Nonprismatic Prestressed UHPC Composite Box Girder with Corrugated Steel Webs. Journal of Bridge Engineering, 28(7). https://doi.org/10.1061/jbenf2.beeng-6038

[IX] Xian, B., Wang, G., Ma, F., Fang, S., Jiang, H., & Xiao, J. (2024). Shear performance of single embedded nut bolted shear connectors in precast steel–UHPC composite beams under combined tension-shear loads. Case Studies in Construction Materials, 21, e03558. https://doi.org/10.1016/j.cscm.2024.e03558

[X] Yang, F., Tu, L., Hu, J., Tan, C., Zou, P., Hu, Z., Qiu, H., & Zhao, H. (2025). Effect of headed stud spacing on flexural behavior of steel plate-UHPC composite beams: Experimental and numerical investigation. Case Studies in Construction Materials, 22, e04403. https://doi.org/10.1016/j.cscm.2025.e04403

[XI] Gyawali, M., Sennah, K., Ahmed, M., & Hamoda, A. (2024). Experimental study of static and fatigue push-out test on headed stud shear connectors in UHPC composite steel beams. Structures, 70, 107923. https://doi.org/10.1016/j.istruc.2024.1079230

[XII] Choi, W., Choi, Y. C., & Yoo, S. W. (2018). Flexural design and analysis of composite beams with inverted-T steel girder and ultra-high-performance concrete slab. *Advances in Civil Engineering*, *2018*, 1356027.

[XIII] Li, G. Q., Li, L., & Li, X. (2011). Experimental and theoretical study on the behavior of steel–concrete composite beams with notched webs of inverted T-shaped steel sections. Advanced Steel Construction, 7(4), 428–446.

[XIV] Shen, J., Zhang, X., Wu, P., Yue, K., & Chen, J. (2025). Experimental and finite element analysis of bending performance of web-embedded double inverted T-shaped steel–concrete composite beams. Buildings, 15(5), 717.

[XV] Farzad, M., Shafieifar, M., & Azizinamini, A. (2019). Experimental and numerical study on bond strength between conventional concrete and ultra-high performance concrete (UHPC). Engineering Structures, 186, 297–305

[XVI] Rana, M. M., Lee, C. K., Al-Deen, S., & Zhang, Y. X. (2018). Flexural behaviour of steel composite beams encased by engineered cementitious composites. Structures, 14, 221–235.

[XVII] Huang, H., Song, J., Gao, X., & Gu, J. (2024). Experimental study on the shear behaviors of inverted castellated T-steel reinforced UHPC (ICTSRU) beams with hollow section. Case Studies in Construction Materials, 21, e03778.

[XVIII] Shoukry, M. S., Fahmy, A. S., Swelem, S. M., & Elgamasy, A. S. (2025). Experimental study on the structural behavior of double Z-shaped steel–encased concrete composite beams. Alexandria Engineering Journal, 128, 1231–1244.

[XIX] Yoo, S.-W., Choi, Y.-C., Choi, J.-H., & Choo, J. F. (2021). Nonlinear flexural analysis of composite beam with Inverted-T steel girder and UHPC slab considering partial interaction. Journal of Building Engineering, 34, 101887.

[XX] Huang, H., Wang, J., & Song, J. (2024). Flexural behavior of composite beams reinforced with I-shaped steel encased in engineered cementitious composite. Buildings, 14(4), 894.

[XXI] Remennikov, A., & Roche, M. (2014). New composite construction of hybrid beams combining steel inverted Tsection and reinforced concrete flange. University of Wollongong.

[XXII] Abubaker, M., Wu, Z., Lin, Z., & Ahmad, M. (2024). Experimental investigation on the flexural behavior of hybrid FRP–steel reinforced ultra-high-performance concrete beams. Construction and Building Materials, 440, 144738.

[XXIII] Chen, Y., Zhang, W., Wang, Y., & Guo, L. (2025). Experimental and numerical study on the shear behavior of steel plate–UHPC composite beams. Case Studies in Construction Materials, 25, e03812.

[XXIV] Li, Y., Zhang, J., Wang, Y., & Yang, L. (2025). Experimental and numerical study on the flexural performance of prefabricated steel–UHPC composite beams with UHPC wedges. Case Studies in Construction Materials, 25, e03884.

[XXV] Al-Abbas, B. H., Alsabbagh, A., Hasan, D. M., Semendary, A. A., & Aaleti, S. (2024). Comparative studies on interfacial bond performance of ultrahigh performance concrete (UHPC) for sustainable repair of bridges and pavements. Results in Engineering, 24, 103525.

[XXVI] Fakeh, M., Jawdhari, A., & Fam, A. (2023). Calibration of ABAQUS Concrete Damage Plasticity (CDP) Model for UHPC Material. Third International Interactive Symposium on Ultra-High Performance Concrete 2023. https://doi.org/10.21838/uhpc.16675

[XXVII] Meng, W., & Khayat, K. H. (2016). Development of Stay-in-Place Formwork Using GFRP Reinforced UHPC Elements. First International Interactive Symposium on UHPC – 2016.

[XXVIII] Dao, C., Mai, V., Vu, N., & Pham, H. (2023). Investigation of the shear behavior of ultra-high performance concrete girder by simulation approach. IOP Conference Series Materials Science and Engineering, 1289(1), 012029. https://doi.org/10.1088/1757-899x/1289/1/012029

[XXIX] Murad, Y. Z., Aljaafreh, A. J., AlMashaqbeh, A., & Alfaouri, Q. T. (2022). Cyclic Behaviour of Heat-Damaged Beam–Column Joints Modified with Nano-Silica, Nano-Titanium, and Nano-Alumina. Sustainability, 14(17), 10916. https://doi.org/10.3390/su141710916